

Magnetoresistance Devices Based on Single Walled Carbon Nanotubes

Oded Hod¹, Eran Rabani¹ and Roi Baer²

¹*School of Chemistry, Tel Aviv University, Tel Aviv. 69978, Israel*

²*Institute of Chemistry and Lise Meitner Center for Quantum Chemistry, the Hebrew University of Jerusalem, Jerusalem 91904 Israel*

(Dated: November 3, 2017)

We demonstrate the physical principles for the construction of a nanometer sized magnetoresistance device based on the Aharonov-Bohm effect. The proposed device is made of a short single-walled carbon nanotube (SWCNT) placed on a substrate and coupled to a tip. We consider conductance due to motion of electrons along the circumference of the tube (as opposed to motion parallel to its axis). We find that the circumference conductance is sensitive to magnetic fields threading the SWCNT due to the Aharonov-Bohm effect, and show that by retracting the tip, so that its coupling to the SWCNT is reduced, very high sensitivity to the threading magnetic field develops. This is due to the formation of a narrow resonance through which the tunneling current flows. Using a bias potential the resonance can be shifted to low magnetic fields, allowing the control of conductance with magnetic fields of the order of 1 Tesla. PACS: 73.63.-b, 73.63.Fg, 75.75.+a

Understanding nanoscale electronic devices is intertwined with the ability to control their properties. One of the most scientifically intriguing and potentially useful property is the control of the electrical conductance in such devices.^{1,2} One convenient way of affecting conductance is by applying magnetic fields. In mesoscopic systems, for example, the conductance is sensitive to the Aharonov-Bohm (AB) effect.³ The study of the interplay between bias and gate voltages, and magnetic fields in these systems has lead to development of micronic AB interferometers.^{4,5,6} At the nanoscale, however, it is widely accepted that AB interferometers do not exist.⁷ This is because unrealistic huge magnetic fields are required to affect conductance through a loop encircling very small areas (for a loop of area A , the magnetic field needed to complete a full AB period can be obtained from the relation $AB = \phi_0$, where $\phi_0 = h/e$ is the flux quantum, h and e are Planck's constant and electron charge, respectively). Thus, at the nanoscale, devices that exhibit large magnetoresistance have been demonstrated based on the Zeeman spin splitting of individual molecular states,⁸ or based on the Kondo effect.⁹

Recently, the AB effect has been measured for single-walled and multi-walled carbon nanotubes (SWCNT and MWCNT, respectively).^{10,11,12} The MWCNT with relatively large diameter (15nm), exhibits h/e -period magnetic flux dependence with $B = 5.8$ Tesla for a full AB period. This result is important, showing that transport is coherent through the tube, in agreement with previous observation.¹³ The measurements for the smaller diameter SWCNT indicate that the band structure of the tube depends on the magnetic flux threading it. But, a full AB period and, thus, switching capability, would require much higher magnetic fields than those used ($B_{max} = 45$ Tesla). Therefore, an open problem is whether SWCNTs, which have been proposed as ideal candidates for the fabrication of nanoelectronic devices,^{14,15,16,17,18,19,20} can exhibit large magnetoresistance (at small magnetic fields) despite the fact that a magnetic field exceeding

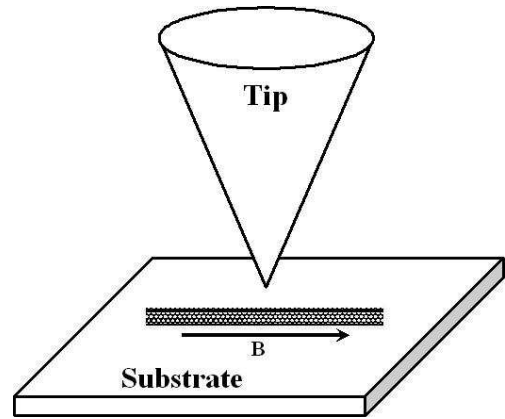


FIG. 1: An illustration of the experimental setup suggested for measuring the cross sectional magnetoresistance of a CNT.

1000 Tesla is required to complete a full AB period for a tube with a diameter comparable to $1nm$.

In this letter, we layout the simple physical principles required to overcome this problem. Utilizing the AB effect, we suggest a way to switch the conductance through the nanometric cross section of a SWCNT by the application of small (≈ 1 Tesla) magnetic fields parallel to the axis of the tube. Our scheme also provides a framework to study and control coherent transport in SWCNTs.

We considered a SWCNT placed on a conducting substrate coupled to a Scanning Tunneling Microscope (STM) tip from above as described schematically in Fig. 1. A bias potential is applied between the STM tip and the underlying surface. We calculate the current through the circumference of the SWCNT (and not along the tube axis). When a magnetic field is applied perpendicular to the cross section of the tube (along its main axis), electron pathways transversing the circular circumference in a clockwise and a counterclockwise manner gain different magnetic phases, and thus AB interfer-

ence occurs.

To calculate the conduction between the STM tip and the substrate in the presence of a magnetic field applied, we have developed a simple approach based on the Magnetic Extended Huckle Theory (MEHT).⁷ Within this approach, we add the proper magnetic terms to the Extended Huckle (tight binding) Hamiltonian, \hat{H}_{EH} (from now on we use atomic units, unless other wise noted):

$$\hat{H} = \hat{H}_{EH} - \mu_B \hat{\mathbf{L}} \cdot \mathbf{B} + \frac{B^2}{8} R_{\perp}^2. \quad (1)$$

Here $\mu_B = \frac{1}{2}$ is the Bohr magneton in atomic units, $\hat{\mathbf{L}}$ is the angular momentum operator, \mathbf{B} is the magnetic field vector, and \mathbf{R}_{\perp} the projection of \mathbf{R} onto the plane perpendicular to \mathbf{B} . A gauge invariant Slater type orbitals (GISTO) basis set is used to evaluate the MEHT Hamiltonian matrix:

$$|GISTO\rangle_{\alpha} = |STO\rangle_{\alpha} e^{-\frac{ie}{\hbar} \mathbf{A}_{\alpha} \cdot \mathbf{r}}, \quad (2)$$

where $|STO\rangle_{\alpha}$ is a Slater type orbital centered on atom α , and \mathbf{A}_{α} is the vector potential evaluated at the nuclear position \mathbf{R}_{α} , $\mathbf{A}_{\alpha} = -\frac{1}{2}(\mathbf{R}_{\alpha} \times \mathbf{B}_{\alpha})$.

For the results reported below, all carbon atoms of the tube were treated explicitly. In the MEHT, each carbon atom contributes two s -electrons and two p -electrons. The valence s and p atomic orbitals are explicitly considered in the Hamiltonian. The STM tip and the contact between the tube and the substrate are modeled by a one dimensional atomistic conducting wire (see more details below). We assume a homogeneous magnetic field parallel to the tube axis and calculate the Hamiltonian matrix elements analytically²¹ within the Pople approximation.²²

The conductance is calculated using the Landauer formalism²³ which relates the conductance to the scattering transmittance probability through the system:

$$g = g_0 \frac{\partial}{\partial V} \int [f_T^{\frac{1}{2}V} - f_S^{-\frac{1}{2}V}] T(E) dE. \quad (3)$$

In the above equation $g_0 = 2e^2/h$ is the quantum conductance, $f_{T/S}^{\pm \frac{1}{2}V}(E) = [1 + e^{\beta(E - \mu_{T/S} \pm \frac{1}{2}V)}]^{-1}$ is the Fermi-Dirac distribution in the STM tip/substrate, $\beta = (k_B T)^{-1}$ is the inverse temperature, $\mu_{T/S}$ is the chemical potential in the STM tip/substrate, and V is the bias potential. We assume that the bias potential across the system drops sharply at both contacts.²⁴ The transmittance $T(E)$ is given by²⁵

$$T = 4tr\{\hat{G}^{\dagger} \Gamma_T \hat{G} \Gamma_S\}. \quad (4)$$

Here, $\Gamma_{T/S}$ is the imaginary absorbing potential representing the imaginary part of the self-energy (Σ) of the STM tip/substrate (we assume that the real part of Σ is zero), and $\hat{G}(E) = [E - \hat{H} + i(\Gamma_T + \Gamma_S)]^{-1}$ is the appropriate Green function. In the following calculations, the imaginary potential was taken in the form of a Gaussian

centered at $b_{T/S}$: $\Gamma_{T/S} = iV_0 \exp\{-\frac{(z-b_{T/S})^2}{2\sigma^2}\}$ where the height of the potential $V_0 \approx \epsilon_F - \epsilon_0$ was approximated by the height of the Fermi energy (ϵ_F) above the valence band bottom (ϵ_0). The width of the absorbing potential was $\sigma \approx 10\text{\AA}$.

In Fig. 2, the conductance through the cross section of a 24x0 SWCNT is plotted against the external axial magnetic field applied. These calculations were done for a tube four unit cells in length. Tests on longer tubes reveal the same qualitative picture described below. We use minimum image periodic boundary conditions for the passivation of the edge atoms. At the inset of the lower panel of Fig. 2, the full AB conductance period is plotted under zero bias voltage and a separation of 2.4Å between the STM tip/substrate and the tube. As can be seen, the full period equals ~ 1500 Tesla, which is expected for an AB interferometer with a radius comparable to 1 nm.

In the upper panel of Fig. 2, we plots the circumference conduction as a function of the axial magnetic field at low values of the field, and for several values of the bias potential. The circumference conduction at zero bias first increases as we switch on the magnetic field (negative magnetoresistance), peaks near $B = 10$ Tesla, and decreases to zero above $B = 30$ Tesla. The maximum conduction observed $g/g_0 = 2$ is limited by our conducting wires. In order to achieve switching capability at magnetic fields smaller than 1 Tesla, it is necessary to move the conduction peak to zero magnetic fields and at the same time reduce the width of this peak.

When a small bias is applied to the sample the conduction peak splits into a doublet. This split can be associated with the specific choice of the potential drop across our system. The position of the corresponding peaks depends on the value of the bias. As can be seen in the figure, by adjusting the bias potential it is possible to shift one of the conductance peaks toward low values of the magnetic field, such that the conductance is maximal at $B = 0$ and positive magnetoresistance is achieved. The shift in the conductance peak can be attributed to the change in the energy level through which conduction occurs when a small bias is applied. As a results of this change, the electron momentum changes and this leads to a shift seen in the conduction peak. We return to this point below when we analyze the results in terms of a simple continuum model.

In the lower panel of Fig. 2 the effect of changing the tube-tip/substrate separation at constant bias potential is studied. As one increases the separation between the tube and the tip/substrate, the coupling between the tube and the tip/substrate decreases, resulting in a reduction of the width of the energy resonances of the SWCNT. Thus, conduction becomes very sensitive to an applied magnetic field and small variations in the field shift the relevant energy level out of resonance. In the magnetoresistance spectrum, this is translated to a narrowing of the transmittance peaks as can be seen in the lower panel of Fig. 2. At the highest separation studied (3.6Å), the width of the conductance peak is comparable

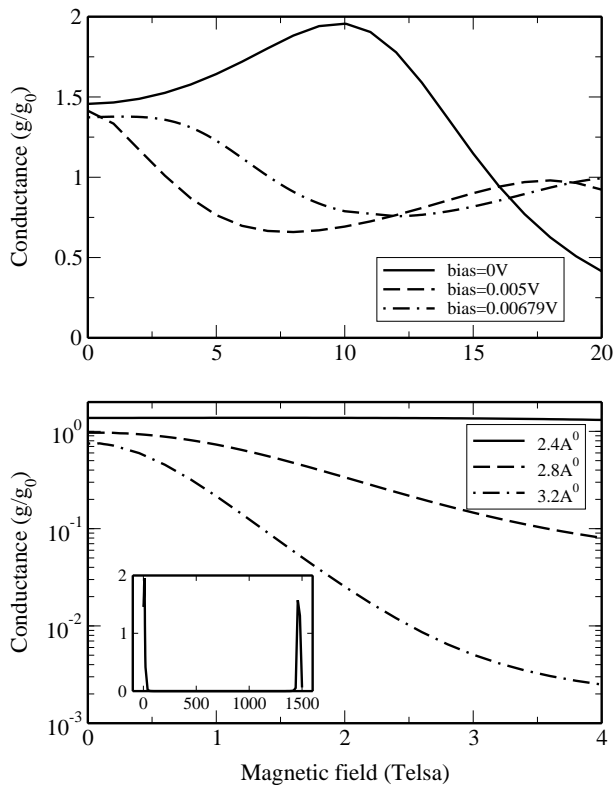


FIG. 2: Conductance versus the magnetic field for a 24x0 SWCNT. Upper panel: The effect of bias potential on the position of the conductance peaks at tube-tip separation of 2.4Å. Lower panel: The effect of increase in the tube-tip separation at a constant bias potential of 0.00679V. Inset: The full AB period for a 24x0 SWCNT at zero bias potential and tube-tip separation of 2.4Å.

to 1 Tesla.

Considering the combined effect of the bias potential and the tube-tip/substrate separation, it is possible to shift the position of the conduction peak to small magnetic fields while at the same time reducing its width. This is achieved by carefully selecting the values of the bias potential and tube-tip/substrate separation. Under proper conditions, we obtain positive magnetoresistance with a sharp response occurring at magnetic fields comparable to 1 Tesla. This result is significant since it implies that despite the fact that the tube radius is small (~ 1 nm) and the corresponding full AB period requires unrealistic large magnetic fields (~ 1500 Tesla), it is possible to achieve magnetic switching at relatively small magnetic fields. This result also agrees with recent experiments that show that the band structure of a carbon nanotube depends on the magnetic flux threading it.¹²

We now turn to analyze the results described above in terms of a simple continuum model. We show that they are reproducible with a single adjustable parameter. Our model includes a cylindrical tube of cross section A coupled to two leads as sketched in the inset of Fig. 3.

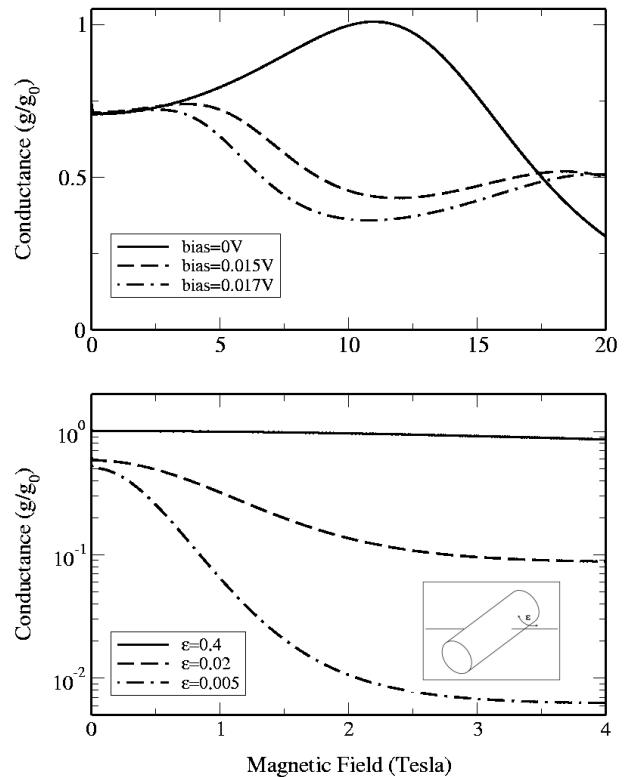


FIG. 3: Conductance versus the magnetic field as computed from the continuum model. The wave length of the Fermi electrons is taken to be $\lambda_F = 2\pi/k_F = 3.522\text{\AA}$ and the diameter of the tube is the same as that of the 24x0 SWCNT (~ 2 nm). Upper panel: For a given value of the junction scattering amplitude $\epsilon = 0.0025$ the application of a bias potential splits the conductance peak and shifts the peaks along the magnetic field axis. Lower panel: At a constant bias voltage (0.0215 V) reducing the scattering parameter results in a narrowing of the transmittance peak. Inset: an illustration of the 1D model setup. The tip and substrate are represented by conducting wires.

The leads mimic the effect of the tip and substrate. A magnetic field of strength B is applied along the tube axis, and the threading magnetic flux is therefore $\phi = AB$.

The transmission probability $T(\phi)$ that a conducting electron with energy E_k originating in the left wire (the STM tip) will pass through the loop and emerge at the right wire (the substrate) can be calculated exactly.^{7,26} Assuming coherent scattering at the incoming and outgoing junctions, we obtain:

$$T(\phi) = T_0 \frac{1 + \cos(2\pi\phi/\phi_0)}{1 + P/R \cos(2\pi\phi/\phi_0) + Q/R \cos(4\pi\phi/\phi_0)}. \quad (5)$$

In the above equation, $T_0 = 32R\epsilon^4 \sin^2(\theta_k)$, as before $\phi_0 = \frac{h}{e}$ is the quantum flux, and P, R, Q are given by $P = 2(c+1)^2[(c-1)^2 - 2(c^2+1)\cos 2\theta_k]$, $R = (c-1)^4 + 4[c^4 + 2c^2 \cos 4\theta_k + 1 - (c^2+1)(c-1)^2 \cos 2\theta_k]$ and $Q =$

$(c+1)^4$ where $c = \sqrt{1-2|\epsilon|^2}$. These coefficients depend on two independent parameters: the amplitude ϵ for an electron to scatter into the tube from the tip, and the spatial phase accumulated by an electron transversing half the circumference of the tube $\theta_k = kL/2$. Here, $k = \sqrt{2m^*E_k/\hbar^2}$ is the wave number of the conducting electron, L is the circumference of the tube, and m^* is the effective mass of the electron. Conduction is obtained by inserting the result for the transmittance (cf. Eq. (5)) into the Landauer formula given by Eq. (3).

In Fig. 3, we plot the conduction calculated for the continuum model. The value of $\theta_k = kL/2$ was calculated with the wave number approximately equal to that of a Fermi electron in a graphene sheet ($k = 2\pi/3.52\text{\AA}^{-1}$), and ϵ was adjusted to reproduce the results for the SWCNT shown in Fig. 2. Analyzing the expression for the transmittance through the tube (cf. Eq. (5)), we find that the position of the conducting peaks depends mainly on the value of (θ_k) . For a maximum conduction at small magnetic fields, $\theta_k = n\pi$, where $n = 1, 2, 3 \dots$. Thus for a given tube circumference L , the wave number of the conducting electrons must satisfy $k = 2\pi n/L$. This is not the case for the parameters chosen above and the maximum conduction occurs at $B = 10$ Tesla. Thus, in order to move the conduction peak to $B = 0$ we apply a bias potential. Introducing a bias potential changes the energy level through which conduction occurs, resulting in a change in the wave number ($k = \sqrt{2m^*E_k/\hbar^2}$) and the spatial angle ($\theta_k = kL/2$). In the upper panel of Fig. 3, we plot the effect of adding a bias potential on the conduction calculated within the continuum model. Similar to the case for the SWCNT shown in the upper panel of Fig. 2, the position of the peaks is sensitive to the value of the bias potential.

In the lower panel of Fig. 3, we plot the conductance for different values of the junction scattering parameter ϵ (the only free parameter in our theory). The value of

the bias potential is chosen such that conduction peaks at zero magnetic field, and positive magnetoresistance is achieved. As can be seen in the figure, the width of the conductance peaks decreases upon a decrease in ϵ . This effect is identical to that observed for SWCNTs when the tube-tip/substrate separation increased. The decrease in ϵ results in a decrease of the width of the energy levels on the tube, since the coupling to the continuum leads is reduced. Thus, for low values of ϵ small magnetic fields are sufficient to move the conducting level out of resonance, and conduction becomes very sensitive to the value of the magnetic field.

The above calculations assume a low temperature of 1 K. However, the effects we report will hold even at higher temperatures. The temperature T must be low enough to resolve the magnetic field splitting of circumference energy levels, and must satisfy $k_B T < [\hbar^2 k_f / m^* D] [\phi / \phi_0]$. Here D is the diameter of the tube, k_f is the Fermi wave number, and m^* is the electron's effective mass. For a ratio of $[\phi / \phi_0] = 1/1500$ (namely, switching capability at 1 Tesla) the upper limit for the temperature is ~ 20 K.

In summary, we have demonstrated that SWCNT can be used as magnetoresistance switching devices based on the AB effect. The essential procedure is to weakly couple the SWCNT to the conducting tip/substrate in order to narrow the conducting resonances, while at the same time to control the position of the resonances by the application of a bias potential. The fact that the diameter of the tube is small becomes beneficial, since the separation between the circumferential energy levels on the tube is large, and conductance can be achieved through a single state.

This work was supported by The Israel Science Foundation (ER) and by the German Israeli Science Foundation (RB).

-
- ¹ A. Nitzan and M. A. Ratner, *Science* **300**, 1384 (2003).
² C. Joachim, J. K. Gimzewski, and A. Aviram, *Nature* **408**, 541 (2000).
³ Y. Aharonov and D. Bohm, *Phys. Rev.* **115**, 485 (1959).
⁴ R. A. Webb, S. Washburn, C. P. Umbach, and R. B. Laibowitz, *Phys. Rev. Lett.* **54**, (1985).
⁵ A. Yacoby, M. Heiblum, D. Mahalu, and H. Shtrikman, *Phys. Rev. Lett.* **74**, 4047 (1995).
⁶ H. R. Shea, R. Martel, and P. Avouris, *Phys. Rev. Lett.* **84**, 4441 (2000).
⁷ O. Hod, R. Baer, and E. Rabani, cond-mat/0406157.
⁸ J. P. and A. N. Pasupathy *et al.*, *Nature* **417**, 722 (2002).
⁹ W. Liang *et al.*, *Nature* **417**, 725 (2002).
¹⁰ A. Bachtold *et al.*, *Nature* **397**, 673 (1999).
¹¹ U. C. Coskun *et al.*, *Science* **304**, 1132 (2004).
¹² S. Zaric *et al.*, *Science* **304**, 1129 (2004).
¹³ W. Liang *et al.*, *Nature* **411**, 665 (2001).
¹⁴ H. J. Dai, E. W. Wong, and C. M. Lieber, *Science* **272**, 523 (1996).
¹⁵ M. Bockrath *et al.*, *Science* **275**, 1922 (1997).
¹⁶ P. G. Collins *et al.*, *Science* **278**, 100 (1997).
¹⁷ M. Menon and D. Srivastava, *J. Mater. Res.* **13**, 2357 (1998).
¹⁸ M. S. Fuhrer *et al.*, *Science* **288**, 494 (2000).
¹⁹ A. Bachtold, P. Hadley, T. Nakanishi, and C. Dekker, *Science* **294**, 1317 (2001).
²⁰ P. Avouris, *Chem. Phys.* **281**, 429 (2002).
²¹ O. Hod, private communication.
²² J. A. Pople, *J. Chem. Phys.* **37**, 53 (1962).
²³ R. Landauer, *IBM J. Res. Dev.* **1**, 223 (1957).
²⁴ S. Pleutin, H. Grabert, G. L. Ingold, and A. Nitzan, *J. Chem. Phys.* **118**, 3756 (2003).
²⁵ R. Baer and D. Neuhauser, *Chem. Phys. Lett.* **374**, 459 (2003).
²⁶ Y. Gefen, Y. Imry, and N. Y. Azbel, *Phys. Rev. Lett.* **52**, 129 (1984).